Academic Platform Journal of Engineering and Science

journal homepage: http://apjes.com/

Immobilization and Characterization of Trypsin on TiO_2 Nanoparticles Activated with Crosslinkers

*[1]Selmihan Sahin, [2]Ismail Ozmen

[1]Suleyman Demirel University, Arts and Sciences Faculty, Department of Chemistry, Cunur, Isparta, 32260, Turkey. selmihansahin@sdu.edu.tr,

[2]Suleyman Demirel University, Arts and Sciences Faculty, Department of Chemistry, Cunur, Isparta, 32260, Turkey. ismailozmen@sdu.edu.tr,

Research Paper Arrival Date: 20.08.2020 Accepted Date: 20.01.2021

Abstract

The immobilization of trypsin (TRP) on the amine-functionalized silica coated TiO_2 nanoparticles (ASTiNPs) with/without different crosslinkers (1,4-phenylene diisothiocyanate (PDC), 1,3-phenylene diisothiocyanate (MDC), glutaraldehyde (GA) has been studied. The ASTiNPs and modified ASTiNPs with the crosslinkers were characterized by FTIR and TEM. When considered the specific activity of immobilized TRP on ASTiNPs, GA-bound TRP showed the higher specific activity. Loading capacity was higher when PDC used as crosslinker. Optimum concentration of the crosslinkers for the TRP immobilization was determined as 20.8 µM of PDC, 5.2 µM of MDC and 1.5 v/v of GA. The direct-bound TRP showed 5% of its initial activity after the four cycles while the GA-bound TRP sustained 7% of its initial activity after the seven cycles and MDC and PDC-bound TRP sustained 7% and 11% of its initial activity after the ten cycles, respectively. The digestion of the Cyt C with immobilized TRP was evaluated by LC-MS/MS analysis. The immobilized TRP on ASTiNPs with crosslinkers showed the higher digestion efficiency of Cyt C when compared to the immobilized TRP on ASTiNPs without crosslinker. Consequently, the PDC-bound TRP on the ASTiNPs gave the better result of digestion efficiency, loading capacity, catalytic activity and reusability than the others.

***Keywords*:** Trypsin, immobilization, crosslinker, amine functionalization, silica coating, TiO_2

1. INTRODUCTION

Immobilization of enzymes offers a number of advantages such as easily recovery from the reaction medium and reusability in continuous processes. However, there are some parameters to be considered for proper immobilization of the enzymes [1]. The one of the important parameters during immobilization is the characteristic properties of the support such as shape, size, chemistry and so on [2].

TiNPs has antimicrobial properties, high mechanical strength, and high corrosion resistance which make them suitable support for enzyme immobilization [3]. However, the loading capacity of biomolecules on these particles is low due to their inorganic characteristic and the presence of insufficient functional groups on their surfaces. Surface modification can be effective to improve their biocompatibility and loading capacity [4]. Surface of TiNPs has been modified with inorganic and organic silane sources to change surface charge, to decrease nanoparticles aggregation, to improve its mechanical and photocatalytic properties and dispersion stability in organic and aqueous media. All of these properties make them more suitable for enzyme immobilization [5]. Previously, Wu et al. [5] have modified the surface of mesoporous TiO_2 with ε-Poly-L-lysine to immobilize negatively charged enzymes and thus, improved their stability and reusability properties. TiNPs were also functionalized with –COOH group using 3-(3,4-dihydroxyphenyl) propionic acid to peroxidase immobilization [6]. 3-APTES has been commonly used in covalent immobilization [7]. It has primary amino group which provides easily modification of the surface of the supports with functional groups as aldehydes, carboxylic acid, isotiyocyanate and epoxy groups [8]. The surface of mesoporous TiO_2 has been chemically modified with 3-aminopropyltriethoxysilane (3-APTES) to immobilize γ-glutamyltranspeptidase and its loading capacity has been increased [9]. However, examples of the silica coating with tetraethyl orthosilicate and then amine functionalization with 3-APTES of the TiNPs (used in the present study) for enzyme immobilization are scarce in the literature. This kind of modifications has been applied on the magnetic nanoparticles [10, 11] and silicon wafers [12].

Crosslinkers can be used for modification of support for efficient immobilization of enzymes. The using of crosslinkers can provide the efficient conversion of the high molecular weight substrate, the changing polarity of the surface causing denaturation, the minimizing undesirable

*Corresponding Author: Suleyman Demirel University, Arts and Sciences Faculty, Department of Chemistry, Cunur, Isparta, 32260, Turkey, selmihansahin@sdu.edu.tr, +902462114340

Doi: 10.21541/apjes.782896

conformational effects and steric hindrance by offering more flexibility which increases catalytic activity of enzymes [3]. The most common crosslinkers used in the literature are dialdehydes or diisothiocyanate which are able to form covalent bonds between enzyme and surface of the supports [13]. Previously, TRP has been immobilized on support with different crosslinkers or directly. These methods have been compared in terms of hydrolytic and synthetic activity [3]. It has been found that immobilized TRP with diaminoalkane, aminoalkanoic acid and biotin crosslinkers have showed higher hydrolytic and synthetic activity compared to the direct-bound TRP. Different from all these studies, the preparation and characterization of the ASTiNPs was described and then TRP was immobilized on them with crosslinkers (GA, PDC, MDC and without crosslinker) to determine the effect of geometry, functional groups (aldehyde and isothiocyanate) and aliphatic and aromatic structure of crosslinkers on the TRP immobilization in this study. The effect of concentration of the crosslinkers on the immobilized TRP activity was examined and compared to a direct-binding method (without crosslinker). Furthermore, the effect of crosslinkers on the catalytic activity and the reusability was investigated and compared with the others. Also, the Cyt C digestion efficiency of the immobilized TRP via GA, PDC, MDC and without crosslinker was investigated by a LC-MS/MS analysis.

2. MATERIALS AND METHODS

2.1. Materials

Benzoyl-L-arginine ethyl ester (BAEE), Cyt C, benzamidine HCL, GA (25%), 3- APTES (98%), and acetonitrile were obtained from Merck. TRP from bovine pancreas was purchased from Amresco Corporation. PDC (98%) and TEOS were purchased from Alfa Aesear. MDC (97%) was purchased from Sigma-Aldrich. Other chemicals and reagents were analytical grade unless otherwise stated.

2.2. Support preparation

2.2.1. Silica coating of TiO_2 surface with TEOS

Preparation of TiNPs was reported in previous article [6]. For silica coating, the sol was first prepared by adding TEOS, 20% ethanol and NH_3 in the glass container and then stirred for 30 min at room temperature. After that, the prepared TiNPs were added to this mixture. It was stirred at 40°C for 12 hours at 80 rpm. The silica-coated TiNPs (STiNPs) were collected by centrifugation at 8000 rpm for 10 min. They were washed with methanol for three times and dried at room temperature for further modifications [10].

The obtained STiNPs were dispersed in ethanol and 3-APTES was added to the suspension to its final concentration 20% w/v, followed by sonication for 30 min. After that, the suspension was incubated at 60 ºC for 12 h under reflux with stirring to provide amine group the surface of the STiNPs. The particles were obtained with centrifugation and then washed with methanol. Finally, they were dried at 50 ºC for 18 h and named as ASTiNPs [10].

2.2.2. Modification of the ASTiNPs with crosslinkers

Modification of ASTiNPs for TRP immobilization was performed with GA, MDC and PDC. The modification was performed according to the procedures with some minor modifications reported by Aissaoui and coworkers [14] for each crosslinker.

1) ASTiNPs: Amine-functionalized STiNPs were used as a support without any modification.
2) GA: ASTiNPs were modified with GA by suspending them in GA solution (in water) and incubated at 25 °C for 2 h. The modified ASTiNPs were washed with distilled water and buffer for three times and dried.
3) MDC: ASTiNPs were modified with MDC solution (in pyridine/DMF, 10%/90%, v/v) at 25 °C for 2 h. The modified samples were washed with acetonitrile for three times and dried.
4) PDC: ASTiNPs were modified with PDC solution (in pyridine/DMF, 10%/90%, v/v) at 25 °C for 2 h and kept away from light. The modified samples were washed with acetonitrile for three times and dried.

2.3. Enzyme immobilization

Firstly, 2 mg/mL of TRP solution containing 0.25 mg/mL benzamidine used as a starting enzyme solution and then, 10 mg of the support was mixed with this solution and incubated for 3 h at 110 rpm and 25°C. Then, the immobilized TRP on the support was washed with KH_2PO_4 buffer 25 mM, pH 6.0. The activity of the immobilized TRP was subsequently determined.
Bradford method was used to determine the amount of immobilized protein by measuring protein concentration of the solutions. The loading capacity (X) was calculated as follow:

$$X= 100x(P_0-P_1-P_2)/W$$

Where P_0 is the protein amount of the initial enzyme solution; P_1 and P_2 are protein amount of the final enzyme solution and the washing solutions, respectively. W is weight of initially added support.

2.4. Activity assay of free and immobilized TRP

Bergmeyer method [15] was used to measure the activity of free and immobilized TRP with slight modifications as fellow: 0.25 mM of BAEE in 67 mM KH_2PO_4 buffer was used as substrate (pH 6.0). The free TRP solution (0.2 mL) was added to 3.0 mL of the substrate solution and the increasing in absorbance of the mixture at 253 nm was measured during 1 min at 25 °C.
The immobilized TRP activity was measured by using 10 mg of TRP immobilized ASTiNPs instead of the enzyme solution. After that, it was incubated at 25ºC for 1 min with gentle shaking and then the immobilized enzyme was

removed by centrifugation. The absorbance of the supernatant was spectrophotometrically measured at 253 nm. One unit of TRP activity was defined as the amount of TRP required for the releasing of 1 µmol Nα-benzoyl-L-arginine from BAEE per minute under the assay conditions [15].

2.5. Characterization

FTIR analyses were measured with a Perkin Elmer Frontier Fourier Transformation Infrared Spectrometer (spectral range between 4000 and 400 cm^{-1}). The characterization of surface morphology of TiNPs, STiNPs and ASTiNPs were performed with the Transmission Electron Microscopy.

2.6. Digestion of Cyt C

Cyt C was used as model protein. To obtain 1 mg/mL of Cyt C solution was prepared in 25 mM KH_2PO_4 (pH 6.0) without any previous treatment [16]. 10 mg of immobilized TRP was added into each tube containing 50 µg of Cyt C for digestion. After incubation at 37 °C, 110 rpm for 15 min, the immobilized TRP was removed from reaction medium, and the supernatant was further analyzed by using LC-MS/MS. For free TRP digestion, free TRP was added into Cyt C solution (1:50 w/w ratio of TRP to protein) and then incubated at 37°C, 110 rpm for 24 h. After incubation, the mixture was further analyzed by using LC-MS/MS [17].

2.7. LC-MS/MS Analysis

The peptides released from the digestion of Cyt C by free TRP and the immobilized TRP with different ways were analyzed LC-MS/MS. Buffer containing 0.1% formic acid, 4 mM ammonium formate and 5% methanol in water was used as mobile phase. MS were obtained in the linear positive mode. The instrument parameters were as follows: positive spray voltage, 3500 V, Sheath gas, 10 Arb, Aux gas, 2 and Sweep gas, 300 and flow rate, 50 µL/min.

3. RESULTS AND DISCUSSION

3.1. Synthesis and characterization of the supports

The immobilization of TRP on TiNPs coated with SiO_2 by TEOS and after amine-grafted with APTES (ASTiNPs) was achieved with four different ways by using crosslinkers, GA, PDC, MDC and without crosslinker. Crosslinkers have different properties such as functional groups (-NCS, -CHO), the connecting chain (aliphatic vs aromatic), and geometrical constraints (meta- vs para- disubstituted aromatics). The schematic representation of the prepared supports by chemical modifications are shown in Figure 1. To confirm the chemical modifications on the surface of TiNPs and the immobilization of TRP, FTIR analysis were performed. FTIR spectra of the TiNPs, STiNPs and ASTiNPs are presented in Figure 2.

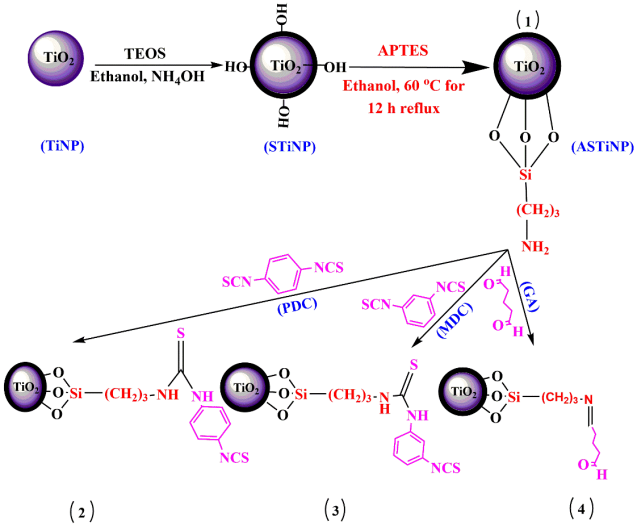

Figure 1. Schematic representation of the chemical modification in the surface of the TiNP and different post modification to obtain support for TRP immobilization.

The spectra of Figure 2a, 2b and 2c display a broad band around 635 cm^{-1} which is due to the vibration of Ti-O-Ti bond. In the spectrum of bare TiO_2 (a), the peak at 3370 cm^{-1} corresponded to –OH groups of weakly chemisorbed and physisorbed water [18]. Also, the absorption bands at 1073, 1223, 2864, 2930 cm^{-1} could be related with C-C-O-stretching vibration and symmetric and asymmetric $–CH_2$ stretching vibration of ethylene glycol which was used in the preparation of the TiO_2.

In the spectrum of STiNPs (Figure 2b), two peaks appeared at 925 cm^{-1} and 1066 cm^{-1} could be relevant to the symmetric and un-symmetric linear stretching vibrations of Si-O-Si bonding [13]. These results indicated that the silica was successfully coated on TiNPs.

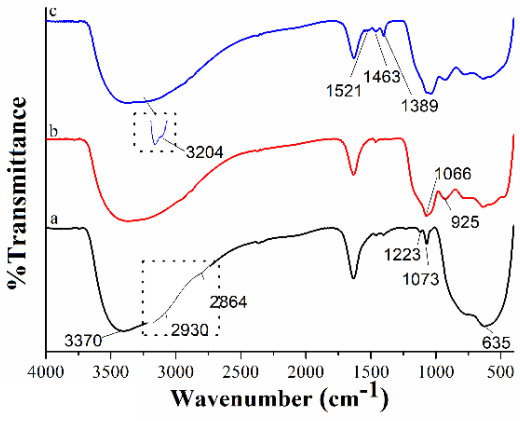

Figure 2. FTIR spectra of the TiNPs (a), STiNPs (b) and ASTiNPs (c).

The introduction of 3-APTES to the surface of STiNPs (ASTiNPs) was confirmed by the deformation vibration adsorption peak of the amine groups appeared at 1463 cm^{-1} and 1521 cm^{-1} [10]. A new peak around 3204 cm^{-1} could be

related to the symmetric stretching modes of NH_2 (Figure 2c). Also, the peak around 1389 cm^{-1} could be assigned to the deformation mode of the Si-CH_2 [19].

The FTIR spectra of the ASTiNPs modified with PDC and its TRP immobilized form (Figure 3). In the spectrum of Figure 3b, the peaks around 1993 and 2180 cm^{-1} could be related with isothiocyanate group [20]. The subsequent immobilization of TRP resulted in the disappearance of these peaks, while a new broad peak appeared at 2089 cm^{-1} (Figure 3c).This peak could be attributed to the characteristic peaks of TRP (Figure 4) and so it suggested that the TRP was successfully immobilized on the ASTiNPs-PDC. Also, the peak around 1560 cm^{-1} in the spectrum of ASTiNPs-PDC (Figure 3b) and ASTiNPs-PDC-E (Figure 3c) assigned to the isothiocyanate group (-N=C=S).

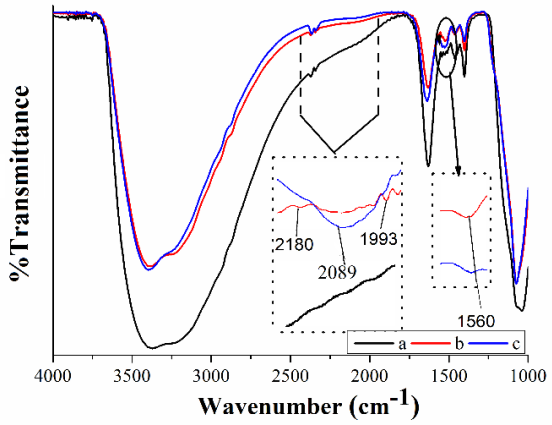

Figure 3. FTIR spectra of the ASTiNPs (a), ASTiNPs-PDC (b) and ASTiNPs-PDC-E (c).

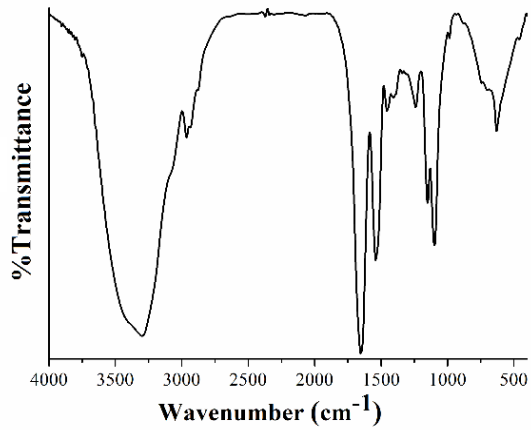

Figure 4. FTIR spectrum of the TRP.

Furthermore, the successful functionalization of the ASTiNPs with MDC was confirmed by the presence of characteristic absorption peak around 2093 cm^{-1} related with isothiocyanate group in the FTIR spectra of the ASTiNPs-MDC (Figure 5b) and ASTiNPs-MDC-E (Figure 5c) [21].
It was found that the –C-N band at 1308 cm^{-1} in the spectra of ASTiNPs-MDC (Figure 5b) and ASTiNPs-MDC-E (Figure 5c) and also a new peak at 1318 cm^{-1} appeared after immobilization of TRP on the ASTiNPs-MDC, indicating the enzyme immobilization (Figure 5c).

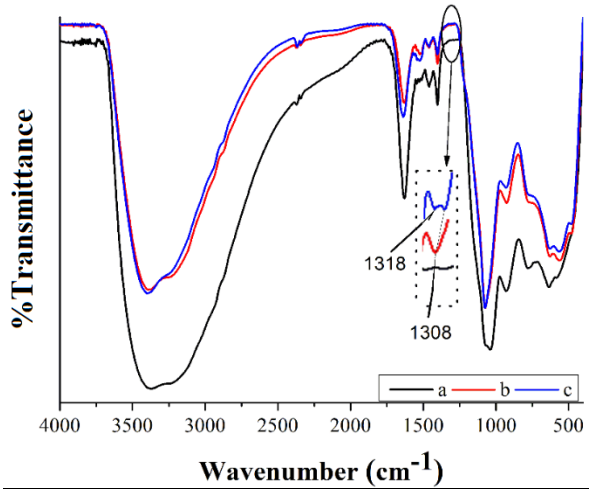

Figure 5. FTIR spectra of the ASTiNPs (a), ASTiNPs-MDC (b) and ASTiNPs-MDC-E (c).

FTIR analysis of ASTiNPs-GA and ASTiNPs-GA-E presented weak new peaks related to N-H bending at 1474 cm^{-1} and 1561 cm^{-1} [22](Figure 6). Furthermore, the decrease in absorption peak at 1463 cm^{-1} related with amine groups (Fig 6a) was observed after binding of GA, indicating the imine bond between the surface amine groups of ASTiNPs aldehyde group in GA [23]. A small shift from 1509 cm^{-1} to 1511 cm^{-1} (Figure 6, inset) could be related with N-H bending (amide II band) [22]. This could confirm that TRP was immobilized onto ASTiNPs-GA successfully.

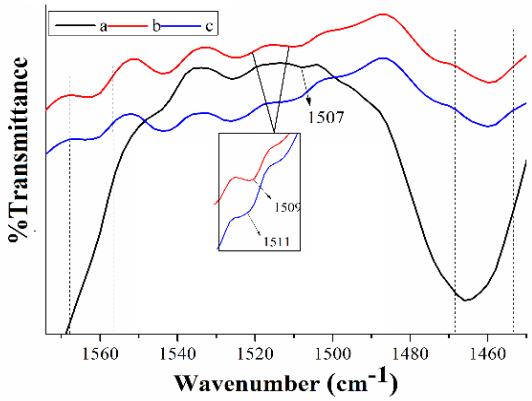

Figure 6. FTIR spectra of the ASTiNPs (a), ASTiNPs-GA (b) and ASTiNPs-GA-E (c).

The morphological features of the prepared TiNPs, STiNPs and ASTiNPs were characterized by using TEM (Figure 7). TEM image of the TiNPs in Figure 7a showed that they were dispersed and there was no aggregation with the average size measured in the range of 65-300 nm. After coating the surface of TiNPs with the silica, the average size of the obtained STiNPs increased about 30 nm (Figure 7b). After amino modification, the ASTiNPs still had almost the same

spherical structures and sizes (Figure 7c). These results were consistent with previous study[24].

3.2. TRP immobilization on the ASTiNPs with different crosslinkers

Table 1 summarizes the specific activities of the immobilized enzyme on ASTiNPs without crosslinker (directly) and with PDC, MDC and GA. The immobilized TRP on ASTiNPs, with GA showed the higher specific activity (968±6 U/mg) than PDC (746±65 U/mg), MDC (598±24 U/mg) and without crosslinker (344±43 U/mg). The conformational effect and steric hindrances could be reduced by attachment of a crosslinker on the support surface. Especially, the using of flexible spacers is assumed to increase the catalytic activity of the enzyme providing free movement [25].

The loading capacity of TRP was the highest (3686±84 mg/g) with PDC used as a crosslinker whereas that was 3266±194 mg/g and 1223±127 mg/g when used MDC and GA as a crosslinkers:, respectively (Table 2). It was decreased to 775±106 mg/g when TRP was directly immobilized on the ASTiNPs. This could be attributed to the hydrophobicity of the surface. LogP values of the PCD, MCD and GA were calculated (https://molinspiration.com/) as 4.67, 4.65 and 1.00, respectively. PDC has the highest hydrophobicity and it also gave the highest loading capacity results. Previously, it has shown that TRP adsorption on the hydrophobic surface is more favorable than the hydrophilic surface, which is consistent with this study [26]. MDC has the almost same LogP value with PDC, however the loading capacity was slightly lower when compared with PDC. It mentioned that MDC caused a degradation on the silanized surface and thus, decreased the amount of immobilized enzyme on the surface [12]. But, in this study the decrease in the loading capacity could be also related with meta- position of the crosslinker [14]. The loading capacity of the ASTiNPs without a crosslinker was as low as in the case of GA used as a crosslinker. This could be attributed to the hydrophilicity of these surfaces [27].

Moreover, when compared ASTiNPs-modified by using different crosslinkers with the supports have been reported in the literature (Table 2), it can be said that ASTiNPs has very high loading capacity even TiO_2 based materials and APTES-modified surfaces. This could be attributed that the silica coating and then amine functionalization the surface of the TiNPs provide more efficient reactive sites with homogeneous distribution to the surface of the TiNPs, thus leading to higher enzyme loading capacity [26]. Also, using crosslinker can provide longer reactive group to the surface of the support, thereby the accessibility of the reactive groups to the more enzyme molecules can be provided in the solution [28]. All tested crosslinkers were short crosslinkers and in the form of X-Spacer-X (X: functional group)[14]. However, among the tested crosslinkers, GA has linear structure (Spacer) which provides more flexibility to the enzyme than PDC and MDC (cyclic spacer). This could explain the highest specific activity of TRP when GA was used as a crosslinker. Although the PDC-bound TRP showed the higher catalytic activity, the higher protein loading capacity of PDC-modified ASTiNPs caused to obtain lower specific activity result.

Table 1. Immobilization of TRP on ASTiNPS

Crosslinkers	Specific activity (U/mg)
Without crosslinker	344±43
GA	968±6
PDC	746±65
MDC	598±24

The influence of crosslinkers concentration on the activity of the immobilized TRP was investigated (Figure 8). All crosslinkers increased the relative activity of the TRP when compared with direct-immobilized TRP on the ASTiNPs (without crosslinker). When PDC was used as a crosslinker, the relative activity of TRP increased and reached the highest value at 20.8 μM and then, decreased (Figure 8a). Otherwise, the relative activity increased significantly with increasing concentration of MDC up to 5.2 μM, in which the maximum value was obtained. With the increased concentration, the relative activity of the immobilized TRP decreased (Figure 8b). As shown in Figure 8c, the relative activity increased obviously when the GA concentration increased from 0 to 1.5 v/v and then decreased and kept almost the same level with a further increase.

The modification of ASTiNPs surface with PDC, MDC and GA were performed to obtain bifunctional supports. The relative activity of the PDC, MDC and GA- bound TRP increased with higher amount of reactive groups on the support with increased concentration of the crosslinkers (PDC, MDC and GA). However, the relative activity values of the immobilized enzymes started to decrease after reached to optimum values. These results showed that the immobilization of TRP on the support surface was increased with modification with crosslinkers and then it was decreased because of the decreasing of the reactive groups on the support with enzyme immobilization [29]. Furthermore, the reactive groups could increase and the length of crosslinker could exceed to certain length with the increased amount of crosslinkers. These might be reasons of decrease in the relative activity above certain concentration of crosslinkers [10, 28]. Another important factor could be the steric hindrance because of the geometry of the crosslinkers (PDC and MDC). Meta- position of the reactive groups on the MDC might lead to decrease in the relative activity of immobilized TRP at lower concentrations according to the PDC [12].

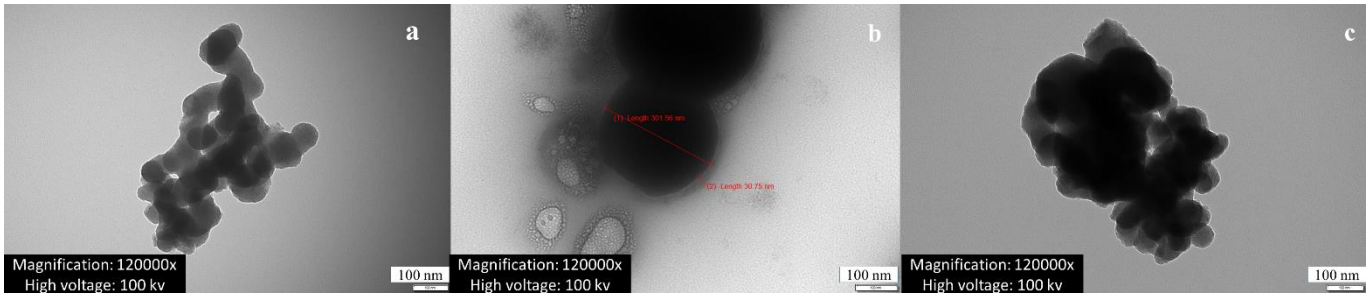

Figure 7. TEM images of the TiNPs (a), STiNPs(b) and ASTiNPs(c)

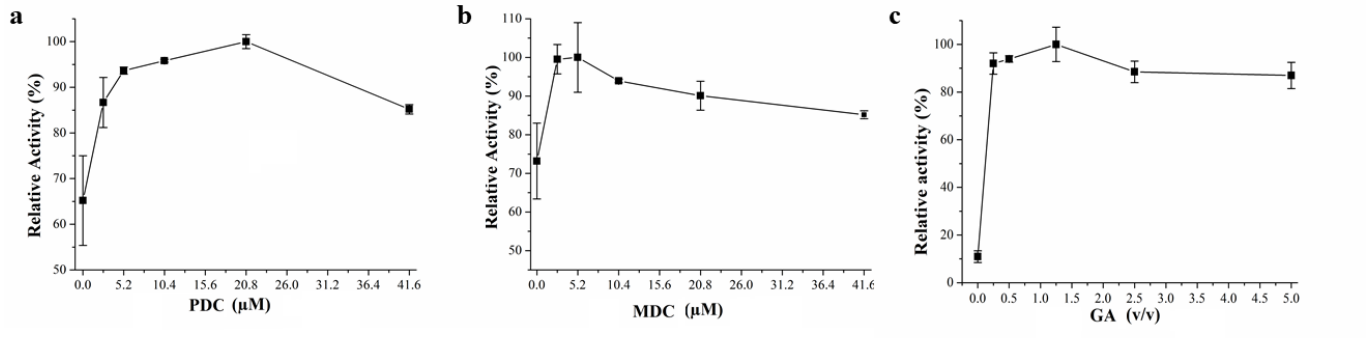

Figure 8. The effect of the concentration of PDC (a), MDC (b) and GA (c) on the relative activity of the immobilized TRP on the ASTiNPs.

Table 2. Protein loading capacity of the different supports reported in the literature.

Enzyme	Support	Crosslinker	Loading capacity (mg/g)	Reference
Laccase	TiO_2	Direct	7.4	[30]
Lysozyme	Mesoporous silica NP	Tannic acid	77.1	[31]
Bovine hemoglobine			396.5	
Bovine serum albumin			130	
Mitochondrial malate dehydrogenase			421	
Laccase	TiO_2-montmorillonite	Direct	35.8	[32]
Cellulase	APTES-Fe_3O_4	GA	176	[33]
Catalase	Reduced graphene oxide−Fe_3O_4	Direct	312.5	[34]
Catalase	Titanate nanotubes coated by poly(dopamine)	Direct	312	[26]
	Titanate nanotubes coated by poly(norepinephrine)		246	
TRP	Magnetic particles	No spacer	0.8 - 59	[3]
		12-aminododecanoic acid	54	
		BSA	13.9	
		Biotin-PEG12	1.2	
TRP	ASTiNPs	Direct	775±106	In this study
		GA	1223±127	
		PDC	3686±84	
		MDC	3266±194	

3.3. LC-MS/MS analysis

To estimate the digestion efficiency of the immobilized TRP with different crosslinkers, a standard protein, namely Cyt C were chosen as substrate and compared with the same sample digested by the classical in solution protocol (24 h digestion, 37 °C). Cyt C can be good indicator for the efficiency of digestion because of its small size and solubility in water (molecular weight of 12 kDa). It is a heme containing protein and has wide applications in biological and biomedical research [35].

Figure 9 shows the LC-MS/MS chromatograms of Cyt C digested by the immobilized TRP with GA, MDC, PDC, without crosslinker on the ASTiNPs and free TRP. The obtained peaks below 400 m/z in all chromotograms were related with the mobile phase and the detection range of peptide fragments were bigger than 500 m/z. Thus, it is needed to consider that the peptide fragments which have m/z value above 500 is important.

From a quantitative point of view, the peptide fragments obtained with the immobilized TRP with GA, MDC, PDC without crosslinker were different. Based on this, the direct-immobilized TRP on the ASTiNPs (without crosslinker, Fig 9d) gave the lowest digestion efficiency while the immobilized TRP with PDC gave the best result than the other crosslinkers even its lower specific activity than GA-bound TRP (Table 1). As aforementioned above, the PDC-bound TRP with had higher catalytic activity provided more efficient digestion of Cyt C. This situation has been explained by Nicoli [36], who has mentioned that the crosslinker increases the mobility of the immobilized enzyme on the surface of the support and thus, the interaction between active sites and target protein can be easily performed. Also, the differences between the results of the crosslinkers could be related with the amount of immobilized enzyme and accessibility of active sites for the substrate [37]. So, it could be said the immobilized TRP with PDC had better accessibility to the cleavage sites of Cyt C as a substrate. The peptide fragments obtained from Cyt C digestion with TRP-bound PDC, MDC and GA were comparable with free TRP in terms of molecular weight and numbers of the fragment. The peak intensity in the chromatogram of the free TRP was higher than the others, but the digestion with free enzyme was performed in 24 h instead of 15 min. This could be attributed to the steric limitations as a result of immobilization [38]. These results demonstrated that the presence of a crosslinkers increased the digestion efficiency when compared to without crosslinker condition and the PDC-bound TRP with gave the better results than the others.

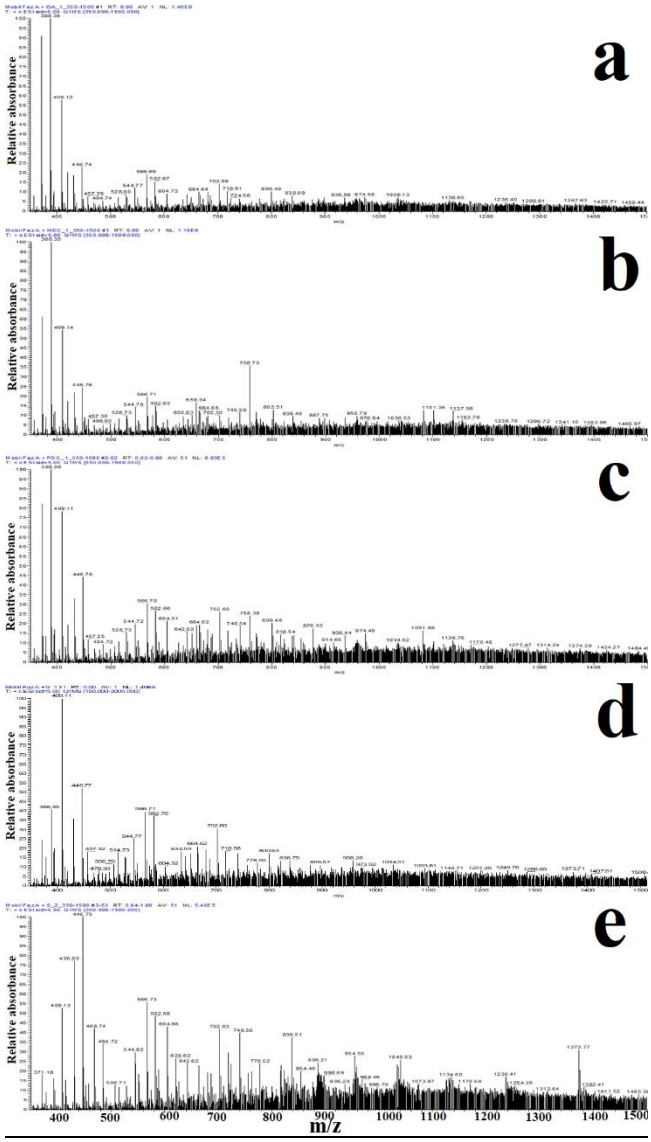

Figure 9. The LC–MS/MS chromatograms of digested Cyt C by immobilized TRP with GA (a), MDC (b), PDC (c), without crosslinker (d) and free TRP (e). Conditions: sample: products of digestion of 1 mg/mL Cyt C, mobil phase 0.1% formic acid, 4 mM ammonium formate and 5% methanol in water MS conditions: spray voltage, 3500 V; sheath gas, 10 Arb; Aux gas, 2 and Sweep gas, 300 and flow rate, 50 μL/min.

3.4. Reusability

One of the important parameters of immobilized enzyme for industrial applications is its reusability in multiple catalytic cycles [39, 40]. Repeated usage of immobilized TRP on ASTiNPS without crosslinker (directly) and with PDC,

MDC and GA were evaluated in batch operation system (Figure 10). The immobilized enzyme was removed from reaction medium by centrifugation and washed with buffer and then used for another fresh reaction medium.

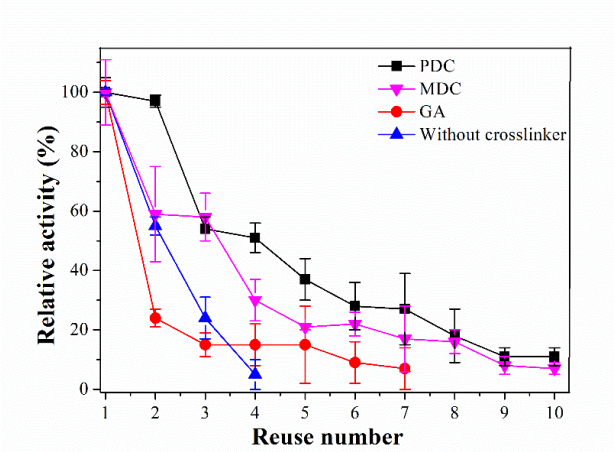

Figure 10. The reusability of the immobilized TRP on ASTiNPS without crosslinker (directly) and with PDC, MDC and GA.

The activity of direct-bound TRP (without crosslinker) remained at 5% after the first four cycles. The rapid loss of activity after four cycles can be explained with enzyme leakage because of physical adsorption of TRP onto the ASTiNPs (without crosslinker) [41, 42]. The reuse number and the percentage of residual activity of the immobilized TRP increased with all tested crosslinkers in comparison with without crosslinker condition. This could be attributed that the immobilization of the protein molecules with crosslinkers such as GA, PDC and MDC might enhance their stability against denaturation by stabilizing their quarternary structure [12, 43].

Using GA as spacer, a sharp decrease to 24% of in initial activity obtained with first cycle, after that the activity remained stable and sustained 7% of its initial activity after the seven cycles. The decrease in the relative activity after the first cycle could be related to the accumulation of final reaction products on the surface of the immobilized TRP [44]. Similar decrease was also obtained when MDC used as crosslinker. When using PDC as crosslinker, the relative activity was higher (11%) after ten reuse cycles in comparison to the using MDC (7%) and GA (7%) as crosslinker. Also, Calvo et al., [7] obtained similar results when used PDC showed higher stability than GA and MDC. Distinctly, the obtained decreasing in the relative activity after seventh cycles could be ascribed to geometry of the crosslinkers. As a result of immobilization via GA, enzyme lost its all-initial activity after seven cycles. This might be related with the hydrophilic character of the GA [45]. Furthermore, geometry of the crosslinkers has an important effect on the activity of enzyme [12]. The other reason of the lower reuse number may be related with that GA has linear structure which provides more flexibility to the protein on the support which may increase denaturation of enzyme [46].

4. CONCLUSION

In present work, the ASTiNPs were prepared and modified with different crosslinkers such as GA, PDC, MDC for immobilization of TRP. The immobilized TRP with these crosslinkers on the ASTiNPs was investigated and compared with direct-bound TRP. The modification of the ASTiNPs with crosslinkers increased the loading capacity of the support and the specific activity of the TRP. The high value of the loading capacity and specific activity was achieved for immobilized TRP on the ASTiNPs modified with PDC. When these result of PDC-bound TRP compared to the others, there was a slight difference with MDC-bound TRP and it was higher than GA-bound TRP. The prepared and modified support has quite high protein loading capacity when compared with the literature (Table 2). Optimum concentration of the crosslinkers for the TRP immobilization was determined as 20.8 µM of PDC, 5.2 µM of MDC and 1.5 v/v of GA. The direct-bound TRP showed 5% of its initial activity after the four cycles while the GA, MDC and PDC-bound TRP sustained 11% of its initial activity after the seven cycles, 7% and 7% of its initial activity after the ten cycles, respectively. The digestion of the Cyt C was evaluated by LC-MS/MS analysis. The presence of a crosslinker increased the digestion efficiency when compared with direct-bound TRP and the immobilized TRP with PDC gave the better digestion efficiency than the others. As a result, the polarity of the crosslinkers has the important effect on the immobilization of TRP on the ASTiNPs while the geometry of the crosslinkers from para- to meta- in PDC and MDC leads to slight difference in the protein loading and the specific activity of the TRP.

REFERENCES

[1] L. Li, H. Li, B. Yan, S. Yu, "Preparation of a reversible soluble-insoluble beta-d-Glucosidase with perfect stability and activity." J Biotechnol, 291, pp. 46-51, 2019.
[2] C. geor malar, M. Seenuvasan, K. S. Kumar, A. Kumar, R. Parthiban, "Review on surface modification of nanocarriers to overcome diffusion limitations: An enzyme immobilization aspect." Biochemical Engineering Journal, 158, pp. 107574, 2020.
[3] J. Andre, D. Saleh, C. Syldatk, R. Hausmann, "Effect of spacer modification on enzymatic synthetic and hydrolytic activities of immobilized trypsin." Journal of Molecular Catalysis B: Enzymatic, 125, pp. 88-96, 2016.
[4] M. G. Miljkovic, V. Lazic, K. Banjanac, S. Z. Davidovic, D. I. Bezbradica, A. D. Marinkovic, D. Sredojevic, J. M. Nedeljkovic, S. I. Dimitrijevic Brankovic, "Immobilization of dextransucrase on functionalized TiO2 supports." Int J Biol Macromol, 114, pp. 1216-1223, 2018.
[5] L. Wu, S. Wu, Z. Xu, Y. Qiu, S. Li, H. Xu, "Modified nanoporous titanium dioxide as a novel carrier for enzyme immobilization." Biosensors and Bioelectronic, 80, pp. 59-66, 2016.
[6] S. Şahin, "Optimization of the Immobilization Conditions of Horseradish Peroxidase on TiO2COOH nanoparticles by Box-Behnken Design." Süleyman Demirel

Üniversitesi Fen Bilimleri Enstitüsü Dergisi, 10.19113/sdufenbed.557021, pp. 904-916, 2019.
[7] J. N.-M. Calvo, M. Elices, G. V. Guinea, J. Pérez-Rigueiro, M. Arroyo-Hernández, "Stability and activity of lactate dehydrogenase on biofunctional layers deposited by activated vapor silanization (AVS) and immersion silanization (IS)." Applied Surface Science, 416, pp. 965-970, 2017.
[8] C. Victor Dos Santos Junior, M. S. Sader, G. C. Goncalves, G. Weissmuller, R. A. Simao, "Effect of pH on the adsorption and interactions of Bovine Serum Albumin with functionalized silicon nitride surface." Colloids Surf B Biointerfaces, 167, pp. 441-447, 2018.
[9] H. Q. Wang, Z. Yao, Y. Sun, Z. Zhou, Q. Xiong, Z. X. Zhong, "Immobilization of γ-glutamyltranspeptidase on silylated mesoporous TiO2 whiskers." Biotechnology and Bioprocess Engineering, 19, pp. 304-310, 2014.
[10] A. H. A. Al-Dhrub, S. Sahin, I. Ozmen, E. Tunca, M. Bulbul, "Immobilization and characterization of human carbonic anhydrase I on amine functionalized magnetic nanoparticles." Process Biochemistry, 57, pp. 95-104, 2017.
[11] E. Aslani, A. Abri, M. Pazhang, "Immobilization of trypsin onto Fe3O4@SiO2 -NH2 and study of its activity and stability." Colloids Surf B Biointerfaces, 170, pp. 553-562, 2018.
[12] N. Aissaoui, L. Bergaoui, S. Boujday, J. F. Lambert, C. Methivier, J. Landoulsi, "Enzyme immobilization on silane-modified surface through short linkers: fate of interfacial phases and impact on catalytic activity." Langmuir, 30, pp. 4066-4077, 2014.
[13] O. Makrygenni, D. Brouri, A. Proust, F. Launay, R. Villanneau, "Immobilization of polyoxometalate hybrid catalysts onto mesoporous silica supports using phenylene diisothiocyanate as a cross-linking agent." Microporous and Mesoporous Materials, 278, pp. 314-321, 2019.
[14] N. Aissaoui, J. Landoulsi, L. Bergaoui, S. Boujday, J. F. Lambert, "Catalytic activity and thermostability of enzymes immobilized on silanized surface: influence of the crosslinking agent." Enzyme Microb Technol, 52, pp. 336-343, 2013.
[15] Bergmeyer H.U., Gawehn K., Grassi M. (1974) Methods of enzymatic analysis., 2nd ed., New York.
[16] Y. Cao, L. Wen, F. Svec, T. Tan, Y. Lv, "Magnetic AuNP@Fe 3 O 4 nanoparticles as reusable carriers for reversible enzyme immobilization." Chemical Engineering Journal, 286, pp. 272-281, 2016.
[17] C. Xia, H. Wang, F. Jiao, F. Gao, Q. Wu, Y. Shen, Y. Zhang, X. Qian, "Rational synthesis of MoS2-based immobilized trypsin for rapid and effective protein digestion." Talanta, 179, pp. 393-400, 2018.
[18] P. M. Kumar, S. Badrinarayanan, M. Sastry, "Nanocrystalline TiO2 studied by optical, FTIR and X-ray photoelectron spectroscopy: correlation to presence of surface states." Thin Solid Films 358, pp. 122-130, 2000.
[19] N. Majoul, S. Aouida, B. Bessaïs, "Progress of porous silicon APTES-functionalization by FTIR investigations." Applied Surface Science, 331, pp. 388-391, 2015.
[20] Lex A., Pacher P., Werzer O., Track A., Shen Q., Schennach R., Koller G., Hlawacek G., Zojer E., Resel R., Ramsey M., Teichert C., Kern W., Trimmel G., "Synthesis of a Photosensitive Thiocyanate-Functionalized Trialkoxysilane and Its Application in Patterned Surface Modifications." Chemistry of Materials, 20, pp. 2009-2015, 2008.
[21] G. Martinez-Edo, M. C. Llinas, S. Borros, D. Sanchez-Garcia, "Isothiocyanate-Functionalized Mesoporous Silica Nanoparticles as Building Blocks for the Design of Nanovehicles with Optimized Drug Release Profile." Nanomaterials (Basel), 9, pp., 2019.
[22] M. Z. Anwar, D. J. Kim, A. Kumar, S. K. S. Patel, S. Otari, P. Mardina, J. H. Jeong, J. H. Sohn, J. H. Kim, J. T. Park, J. K. Lee, "SnO2 hollow nanotubes: a novel and efficient support matrix for enzyme immobilization." Sci Rep, 7, pp. 15333, 2017.
[23] P. Saengdee, W. Chaisriratanakul, W. Bunjongpru, W. Sripumkhai, A. Srisuwan, W. Jeamsaksiri, C. Hruanun, A. Poyai, C. Promptmas, "Surface modification of silicon dioxide, silicon nitride and titanium oxynitride for lactate dehydrogenase immobilization." Biosens Bioelectron, 67, pp. 134-138, 2015.
[24] D. Liu, A. M. Pourrahimi, L. K. H. Pallon, R. L. Andersson, M. S. Hedenqvist, U. W. Gedde, R. T. Olsson, "Morphology and properties of silica-based coatings with different functionalities for Fe3O4, ZnO and Al2O3 nanoparticles." RSC Advances, 5, pp. 48094-48103, 2015.
[25] C. Daglioglu, F. Zihnioglu, "Covalent immobilization of trypsin on glutaraldehyde-activated silica for protein fragmentation." Artif Cells Blood Substit Immobil Biotechnol, 40, pp. 378-384, 2012.
[26] D. Yang, X. Wang, Q. Ai, J. Shi, Z. Jiang, "Performance comparison of immobilized enzyme on the titanate nanotube surfaces modified by poly(dopamine) and poly(norepinephrine)." RSC Advances, 5, pp. 42461-42467, 2015.
[27] B. Niu, B. Li, H. Wang, R. Guo, H. Liang, M. Qiao, W. Li, "Preparing bioactive surface of polystyrene with hydrophobin for trypsin immobilization." Materials Research Express, 3, pp. 055402, 2016.
[28] S. Sahin, I. Ozmen, "Determination of optimum conditions for glucose-6-phosphate dehydrogenase immobilization on chitosan-coated magnetic nanoparticles and its characterization." Journal of Molecular Catalysis B: Enzymatic, 133, pp. S25-S33, 2016.
[29] B. Tural, T. Tarhan, S. Tural, "Covalent immobilization of benzoylformate decarboxylase from Pseudomonas putida on magnetic epoxy support and its carboligation reactivity." Journal of Molecular Catalysis B: Enzymatic, 102, pp. 188-194, 2014.
[30] C. Ji, L. N. Nguyen, J. Hou, F. I. Hai, V. Chen, "Direct immobilization of laccase on titania nanoparticles from crude enzyme extracts of P. ostreatus culture for micro-pollutant degradation.", 178, pp. 215-223, 2017.
[31] Z. Gao, I. Zharov, "Large Pore Mesoporous Silica Nanoparticles by Templating with a Nonsurfactant Molecule, Tannic Acid." Chemistry of Materials, 26, pp. 2030-2037, 2014.

[32] Q. Wang, L. Peng, G. Li, P. Zhang, D. Li, F. Huang, Q. Wei, "Activity of laccase immobilized on TiO2-montmorillonite complexes." Int J Mol Sci, 14, pp. 12520-12532, 2013.
[33] J. Jia, W. Zhang, Z. Yang, X. Yang, N. Wang, X. Yu, "Novel Magnetic Cross-Linked Cellulase Aggregates with a Potential Application in Lignocellulosic Biomass Bioconversion." Molecules, 22, pp., 2017.
[34] D. Yang, X. Wang, J. Shi, X. Wang, S. Zhang, P. Han, Z. Jiang, "In situ synthesized rGO–Fe3O4 nanocomposites as enzyme immobilization support for achieving high activity recovery and easy recycling." Biochemical Engineering Journal, 105, pp. 273-280, 2016.
[35] K. Atacan, A. N. Kursunlu, M. Ozmen, "Preparation of pillar[5]arene immobilized trypsin and its application in microwave-assisted digestion of Cytochrome c." Mater Sci Eng C Mater Biol Appl, 94, pp. 886-893, 2019.
[36] R. Nicoli, N. Gaud, C. Stella, S. Rudaz, J. L. Veuthey, "Trypsin immobilization on three monolithic disks for on-line protein digestion." J Pharm Biomed Anal, 48, pp. 398-407, 2008.
[37] C. Temporini, E. Perani, F. Mancini, M. Bartolini, E. Calleri, D. Lubda, G. Felix, V. Andrisano, G. Massolini, "Optimization of a trypsin-bioreactor coupled with high-performance liquid chromatography-electrospray ionization tandem mass spectrometry for quality control of biotechnological drugs." J Chromatogr A, 1120, pp. 121-131, 2006.
[38] C. Rocha, M. P. Gonçalves, J. A. Teixeira, "Immobilization of trypsin on spent grains for whey protein hydrolysis." Process Biochemistry, 46, pp. 505-511, 2011.
[39] P. Zucca, E. Sanjust, "Inorganic materials as supports for covalent enzyme immobilization: methods and mechanisms." Molecules, 19, pp. 14139-14194, 2014.
[40] A. B. Jarzębski, K. Szymańska, J. Bryjak, J. Mrowiec-Białoń, "Covalent immobilization of trypsin on to siliceous mesostructured cellular foams to obtain effective biocatalysts." Catalysis Today, 124, pp. 2-10, 2007.
[41] R. Abdulla, S. A. Sanny, E. Derman, "Stability studies of immobilized lipase on rice husk and eggshell membrane." IOP Conference Series: Materials Science and Engineering, 206, pp. 012032, 2017.
[42] S. Zhang, Q. Deng, Y. Li, M. Zheng, C. Wan, C. Zheng, H. Tang, F. Huang, J. Shi, "Novel amphiphilic polyvinylpyrrolidone functionalized silicone particles as carrier for low-cost lipase immobilization." R Soc Open Sci, 5, pp. 172368, 2018.
[43] Y. A. Duman, N. Tekin, "Kinetic and thermodynamic properties of purified alkaline protease from Bacillus pumilus Y7 and non-covalent immobilization to poly(vinylimidazole)/clay hydrogel." Engineering in Life Sciences, 20, pp. 36-49, 2019.
[44] J. A. Torres, M. C. Silva, J. H. Lopes, A. E. Nogueira, F. G. E. Nogueira, A. D. Correa, "Development of a reusable and sustainable biocatalyst by immobilization of soybean peroxidase onto magnetic adsorbent." Int J Biol Macromol, 114, pp. 1279-1287, 2018.
[45] L. J. Li, W. J. Xia, G. P. Ma, Y. L. Chen, Y. Y. Ma, "A study on the enzymatic properties and reuse of cellulase immobilized with carbon nanotubes and sodium alginate." AMB Express, 9, pp. 112, 2019.
[46] C. Bonzom, L. Schild, H. Gustafsson, L. Olsson, "Feruloyl esterase immobilization in mesoporous silica particles and characterization in hydrolysis and transesterification." BMC Biochem, 19, pp. 1, 2018.